*Research Article*

# Reconstruction of Sensory Stimuli Encoded with Integrate-and-Fire Neurons with Random Thresholds

**Aurel A. Lazar and Eftychios A. Pnevmatikakis**

*Department of Electrical Engineering, Columbia University, New York, NY 10027, USA*

Correspondence should be addressed to Eftychios A. Pnevmatikakis, eap2111@columbia.edu

We present a general approach to the reconstruction of sensory stimuli encoded with leaky integrate-and-fire neurons with random thresholds. The stimuli are modeled as elements of a Reproducing Kernel Hilbert Space. The reconstruction is based on finding a stimulus that minimizes a regularized quadratic optimality criterion. We discuss in detail the reconstruction of sensory stimuli modeled as absolutely continuous functions as well as stimuli with absolutely continuous first-order derivatives. Reconstruction results are presented for stimuli encoded with single as well as a population of neurons. Examples are given that demonstrate the performance of the reconstruction algorithms as a function of threshold variability.

## 1. Introduction

Formal spiking neuron models, such as integrate-and-fire (IAF) neurons, encode information in the time domain [1]. Assuming that the input signal is bandlimited and the bandwidth is known, a perfect recovery of the stimulus based upon the spike times can be achieved provided that the spike density is above the Nyquist rate [2]. These results hold for a wide variety of sensory stimuli, including audio [3] and video [4], encoded with a population of IAF neurons. More generally, Time Encoding Machines (TEMs) encode analog amplitude information in the time domain using only asynchronous circuits [2]. Time encoding has been shown to be closely related to traditional amplitude sampling. This observation has enabled the application of a large number of recovery results obtained for signals encoded using irregular sampling to time encoding.

A common underlying assumption of TEM models is that the input stimulus is bandlimited with known bandwidth. Implicit in this assumption is that the signal is defined on the entire real line. In sensory systems, however, the bandwidth of the signal entering the soma of the neuron is often unknown. Ordinarily good estimates of the bandwidth are not available due to nonlinear processing in the upstream transduction pathways, for example, contrast extraction in vision. In addition, stimuli have limited time support and the neurons respond with a finite number of spikes.

Furthermore, neuronal spike trains exhibit variability in response to identical input stimuli. In simple formal spiking neuron models, such as IAF neurons, this variability is associated with random thresholds [5]. IAF neurons with random thresholds have been used to model the observed spike variability of certain neurons of the fly visual system [6]. Linear recovery methods were proposed in [7] for an ideal IAF neuron with exponentially distributed thresholds that exhibits Poisson statistics.

A perfect recovery of a stimulus encoded with a formal neuron model with random threshold along the lines of [3] is not possible, and an alternative reconstruction formalism is needed. Consequently, a major goal is the development of a mathematical framework for the representation and recovery of arbitrary stimuli with a population of neurons with random thresholds on finite time intervals. There are two key elements to such an extension. First, the signal model is defined on a finite time interval and, therefore, the bandlimited assumption does not hold. Second, the number of degrees of freedom in signal reconstruction is reduced

by either introducing a natural signal recovery constraint [8] or by assuming that the stimuli are restricted to be "smooth."

In this paper, we propose a Reproducing Kernel Hilbert Space (RKHS) [9] framework for the representation and recovery of finite length stimuli with a population of leaky integrate-and-fire (LIF) neurons with random thresholds. More specifically, we set up the recovery problem as a regularized optimization problem, and use the theory of smoothing splines in RKHS [10] to derive an optimal (nonlinear) solution.

RKHSs play a major role in statistics [10] and in machine learning [11]. In theoretical neuroscience they have been little used with the exception of [12]. In the latter work, RKHSs have been applied in a probabilistic setting of point process models to study the distance between spike trains of neural populations. Spline models have been used in computational neuroscience in the context of estimating the (random) intensity rate from raster neuron recordings [13, 14]. In this paper we will bring the full power of RKHSs and the theory of smoothing splines to bear on the problem of reconstruction of stimuli encoded with a population of IAF neurons with random thresholds.

Although the methodology employed here applies to arbitrary RKHSs, for example, space of bandlimited stimuli, we will focus in this paper on Sobolev spaces. Signals in Sobolev spaces are rather natural for modeling purposes as they entail absolutely continuous functions and their derivatives. A more precise definition will be given in the next section. The inner-product in Sobolev spaces is based on higher-order function derivatives. In the RKHS of bandlimited functions, the inner-product formulation of the $t$-transform is straightforward because of the simple structure of the inner-product in these space [3, 4]. However this is not the case for Sobolev spaces, since the inner-product has a more complex structure. We will be interpreting the $t$-transform as a linear functional on the Sobolev space, and then through the use of the Riesz representation theorem, rewrite it in an inner-product form that is amenable to further analytical treatment. We can then apply the key elements of the theory developed in [10].

This paper is organized as follows. In Section 2 the problem of representation of a stimulus defined in a class of Sobolev spaces and encoded by leaky integrate-and-fire (LIF) neurons with random thresholds is formulated. In Section 3 the stimulus reconstruction problem is addressed when the stimuli are encoded by a single LIF neuron with random threshold. The reconstruction algorithm calls for finding a signal that minimizes a regularized optimality criterion. Reconstruction algorithms are worked out in detail for the case of absolutely continuous stimuli as well as stimuli with absolutely continuous first-order derivatives. Two examples are described. In the first, the recovery of a stimulus from its temporal contrast is given. In the second, the recovery of stimuli encoded with a pair of rectifier neurons is presented. Section 4 generalizes the previous results to stimuli encoded with a population of LIF neurons. The paper concludes with Section 5.

## 2. Encoding of Stimuli with LIF Neurons with Random Thresholds

In this section we formulate the problem of stimulus encoding with leaky integrate-and-fire neurons with random thresholds. The stimuli under consideration are defined on a finite time interval and are assumed to be functions that have a smoothness property. The natural mathematical setting for the stimuli considered in this paper is provided by function spaces of the RKHS family [15]. A brief introduction to RKHSs is given in Appendix A.1.

We show that encoding with LIF neurons with random thresholds is akin to taking a set of noisy measurements on the stimulus. We then demonstrate that these measurements can be represented as projections of the stimulus on a set of sampling functions.

*2.1. Modeling of Sensory Stimuli as Elements of RKHSs.* There is a rich collection of Reproducing Kernel Hilbert Spaces that have been thoroughly investigated and the modeler can take advantage of [9]. In what follows we restrict ourselves to a special class of RKHSs, the so-called Sobolev spaces [16]. Sobolev spaces are important because they combine the desirable properties of important function spaces (e.g., absolute continuous functions, absolute continuous derivatives, etc.), while they retain the reproducing property. Moreover a parametric description of the space (e.g., bandwidth) is not required.

Stimuli are functions $u = u(t)$, $t \in \mathcal{T}$, defined as elements of a Sobolev space $\mathcal{S}_m = \mathcal{S}_m(\mathcal{T})$, $m \in \mathbb{N}^*$. The Sobolev space $\mathcal{S}_m(\mathcal{T})$, for a given $m$, $m \in \mathbb{N}^*$, is defined as

$$\mathcal{S}_m = \left\{ u \mid u, u', \dots, u^{(m-1)} \text{ absolutely continuous}, u^{(m)} \in L^2(\mathcal{T}) \right\}, \tag{1}$$

where $L^2(\mathcal{T})$ is the space of functions of finite energy over the domain $\mathcal{T}$. We will assume that the domain $\mathcal{T}$ is a finite interval on $\mathbb{R}$ and, w.l.o.g, we set it to $\mathcal{T} = [0, 1]$. Note that the space $\mathcal{S}_m$ can be written as $\mathcal{S}_m := \mathcal{H}_0 \oplus \mathcal{H}_1$ ($\oplus$ denotes the direct sum) with

$$\mathcal{H}_0 := \mathrm{span}\{1, t, \dots, t^{m-1}\},$$

$$\mathcal{H}_1 := \Big\{ u \mid u \in \mathcal{C}^{m-1}(\mathcal{T}),\ u^{(m)} \in \mathcal{L}_2(\mathcal{T}), \tag{2}$$

$$u(0) = u'(0) = \cdots = u^{(m-1)}(0) = 0 \Big\},$$

where $\mathcal{C}^{m-1}(\mathcal{T})$ denotes the space of $m-1$ continuously differentiable functions defined on $\mathcal{T}$. It can be shown [9] that the space $\mathcal{S}_m$ endowed with the inner-product $\langle \cdot, \cdot \rangle : \mathcal{S}_m \times \mathcal{S}_m \mapsto \mathbb{R}$ given by

$$\langle u, v \rangle := \sum_{i=0}^{m-1} u^{(i)}(0) v^{(i)}(0) + \int_0^1 u^{(m)}(s) v^{(m)}(s)\, ds \tag{3}$$

is an RKHS with reproducing kernel

$$K(s, t) = \sum_{i=1}^{m} \chi_i(s)\chi_i(t) + \int_0^1 G_m(s, \tau) G_m(t, \tau)\, d\tau, \tag{4}$$

with $\chi_i(t) = t^{i-1}/(i-1)!$ and $G_m(t,s) = (t-s)_+^{m-1}/(m-1)!$. Note that the reproducing kernel of (4) can be written as $K(s,t) = K^0(s,t) + K^1(s,t)$ with

$$K^0(s,t) = \sum_{i=1}^{m} \chi_i(s)\chi_i(t),$$

$$K^1(s,t) = \int_0^1 G_m(s,\tau)G_m(t,\tau)\, d\tau. \tag{5}$$

The kernels $K^0$, $K^1$ are reproducing kernels for the spaces $\mathcal{H}_0$, $\mathcal{H}_1$ endowed with inner products given by the two terms on the right-hand side of (3), respectively. Note also that the functions $\chi_i(t)$, $i = 1, 2, \ldots, m$, form an orthogonal base in $\mathcal{H}_0$.

*Remark 1.* The norm and the reproducing kernel in an RKHS uniquely determine each other. For examples of Sobolev spaces endowed with a variety of norms, see [9].

### 2.2. Encoding of Stimuli with a LIF Neuron.
Let $u = u(t)$, $t \in \mathcal{T}$, denote the stimulus. The stimulus biased by a constant background current $b$ is fed into a LIF neuron with resistance $R$ and capacitance $C$. Furthermore, the neuron has a random threshold with mean $\delta$ and variance $\sigma^2$. The value of the threshold changes only at spike times, that is, it is constant between two consecutive spikes. Assume that after each spike the neuron is reset to the initial value zero. Let $(t_k)$, $k = 1, 2, \ldots, n+1$, denote the output spike train of the neuron. Between two consecutive spike times the operation of the LIF neuron is fully described by the $t$-transform [1]

$$\int_{t_k}^{t_{k+1}} (b + u(s)) \exp\left(-\frac{t_{k+1} - s}{RC}\right) ds = C\delta_k, \tag{6}$$

where $\delta_k$ is the value of the random threshold during the interspike interval $[t_k, t_{k+1})$. The $t$-transform can also be rewritten as

$$L_k u = q_k + \varepsilon_k, \tag{7}$$

where $L_k : \mathcal{S}_m \mapsto \mathbb{R}$ is a linear functional given by

$$L_k u = \int_{t_k}^{t_{k+1}} u(s) \exp\left(-\frac{t_{k+1} - s}{RC}\right) ds,$$

$$q_k = C\delta - bRC\left(1 - \exp\left(-\frac{t_{k+1} - t_k}{RC}\right)\right), \tag{8}$$

$$\varepsilon_k = C(\delta_k - \delta),$$

and the $\varepsilon_k$'s are i.i.d. random variables with mean zero and variance $(C\sigma)^2$ for all $k = 1, 2, \ldots, n$. The sequence $(L_k)$, $k = 1, 2, \ldots, n$, has a simple interpretation; it represents the set of $n$ measurements performed on the stimulus $u$.

**Lemma 1.** *The $t$-transform of the LIF neuron can be written in inner-product form as*

$$\langle \phi_k, u \rangle = q_k + \varepsilon_k, \tag{9}$$

where

$$\phi_k(t) = \int_{t_k}^{t_{k+1}} K(t,s) \exp\left(-\frac{t_{k+1} - s}{RC}\right) ds, \tag{10}$$

$q_k$, $\varepsilon_k$ are given by (8), $k = 1, 2, \ldots, n$, and $\langle \cdot, \cdot \rangle$ is the inner-product (3) for the space $\mathcal{S}_m$, $m \in \mathbb{N}$. In addition the $\varepsilon_k$'s are i.i.d. random variables with mean zero and variance $(C\sigma)^2$ for all $k = 1, 2, \ldots, n$.

*Proof.* We will rewrite the linear functionals of (7) in inner-product form, that is, as projections in $\mathcal{S}_m$. The existence of an inner-product form representation is guaranteed by the Riesz lemma (see Appendix A.2). Thus, there exists a set of functions $\phi_k \in \mathcal{S}_m$, such that

$$L_k u = \langle \phi_k, u \rangle, \tag{11}$$

for all $k = 1, 2, \ldots, n$. Since $\mathcal{S}_m$ is a RKHS, we also have that

$$\phi_k(t) = \langle \phi_k, K_t \rangle = L_k K_t = \int_{t_k}^{t_{k+1}} K(t,s) \exp\left(-\frac{t_{k+1} - s}{RC}\right) ds, \tag{12}$$

where $K_t(\cdot) = K(\cdot, t)$, for all $t \in \mathcal{T}$. $\qquad\square$

The main steps of the proof of Lemma 1 are schematically depicted in Figure 1. The $t$-transform has an equivalent representation as a series of linear functionals acting on the stimulus $u$. These functionals are in turn represented as projections of the stimulus $u$ on a set of functions in the space $\mathcal{S}_m$.

### 2.3. Encoding of Stimuli with a Population of LIF Neurons.
In this section we briefly discuss the encoding of stimuli with a population of LIF neurons with random thresholds. The presentation follows closely the one in Section 2.2. The main result obtained in Lemma 2 will be used in Section 4.

Consider a population of $N$ LIF neurons where neuron $j$ has a random threshold with mean $\delta^j$ and standard deviation $\sigma^j$, bias $b^j$, resistance $R^j$, and capacitance $C^j$. Whenever the membrane potential reaches its threshold value, the neuron $j$ fires a spike and resets its membrane potential to 0. Let $t_k^j$ denote the $k$th spike of neuron $j$, with $k = 1, 2, \ldots, n_j + 1$. Here $n_j + 1$ denotes the number of spikes that neuron $j$ triggers, $j = 1, 2, \ldots, N$.

The $t$-transform of each neuron $j$ is given by (see also (6))

$$\int_{t_k^j}^{t_{k+1}^j} \left(b^j + u(s)\right) \exp\left(-\frac{t_{k+1}^j - s}{R^j C^j}\right) ds = C^j \delta_k^j, \tag{13}$$

for all $k = 1, 2, \ldots, n_j$, and $j = 1, 2, \ldots, N$.

**Lemma 2.** *The $t$-transform of the LIF population can be written in inner-product form as*

$$\left\langle \frac{1}{C^j \sigma^j} \phi_k^j, u \right\rangle = \frac{1}{C^j \sigma^j} q_k^j + \varepsilon_k^j, \tag{14}$$
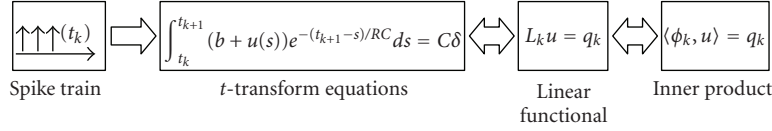
FIGURE 1: The operator interpretation of stimulus encoding with a LIF neuron.

with $\phi_k^j$, $q_k^j$ essentially given by (10), (8) (plus an added superscript $j$), and

$$\varepsilon_k^j = \frac{\delta_k^j - \delta^j}{\sigma^j} \qquad (15)$$

are i.i.d. random variables with mean zero and variance one for all $k = 1, 2, \ldots, n_j$, and $j = 1, 2, \ldots, N$.

*Proof.* Largely the same as the proof of Lemma 1.     □

## 3. Reconstruction of Stimuli Encoded with a LIF Neuron with Random Threshold

In this section we present in detail the algorithm for the reconstruction of stimuli encoded with a LIF neuron with random threshold. Two cases are considered in detail. First, we provide the reconstruction of stimuli that are modeled as absolutely continuous functions. Second, we derive the reconstruction algorithm for stimuli that have absolutely continuous first-order derivatives. The reconstructed stimulus satisfies a regularized optimality criterion. Examples that highlight the intuitive properties of the results obtained are given at the end of this section.

*3.1. Reconstruction of Stimuli in Sobolev Spaces.* As shown in Section 2.2, a LIF neuron with random threshold provides the reader with the set of measurements

$$\langle \phi_k, u \rangle = q_k + \varepsilon_k, \qquad (16)$$

where $\phi_k \in \mathcal{S}_m$ for all $k = 1, 2, \ldots, n$. Furthermore, $(\varepsilon_k)$, $k = 1, 2, \ldots, n$, are i.i.d. random variables with zero mean and variance $(C\sigma)^2$.

An optimal estimate $\hat{u}$ of $u$ minimizes the cost functional

$$\frac{1}{n} \sum_{k=1}^{n} (q_k - \langle \phi_k, u \rangle)^2 + \lambda \| \mathcal{P}_1 u \|^2, \qquad (17)$$

where $\mathcal{P}_1 : \mathcal{S}_m \mapsto \mathcal{H}_1$ is the projection of the Sobolev space $\mathcal{S}_m$ to $\mathcal{H}_1$. Intuitively, the nonnegative parameter $\lambda$ regulates the choice of the estimate $\hat{u}$ between faithfulness to data fitting ($\lambda$ small) and maximum smoothness of the recovered signal ($\lambda$ large). We further assume that the threshold of the neuron is modeled as a sequence of i.i.d. random variables $(\delta_k)$, $k = 1, 2, \ldots, n$, with Gaussian distribution with mean $\delta$ and variance $\sigma^2$. Consequently, the random variables $(\varepsilon_k)$, $k = 1, 2, \ldots, n$, are i.i.d. Gaussian with mean zero and variance $(C\sigma)^2$. Of main interest is the effect of random threshold fluctuations for $\sigma \ll \delta$. (Note that for $\sigma \ll \delta$ the probability that the threshold is negative is close to zero). We have the following theorem.

**Theorem 1.** *Assume that the stimulus $u = u(t)$, $t \in [0, 1]$, is encoded into a time sequence $(t_k)$, $k = 1, 2, \ldots, n$, with a LIF neuron with random threshold that is fully described by (6). The optimal estimate $\hat{u}$ of $u$ is given by*

$$\hat{u} = \sum_{i=1}^{m} d_i \chi_i + \sum_{k=1}^{n} c_k \psi_k, \qquad (18)$$

*where*

$$\chi_i(t) = \frac{t^{i-1}}{(i-1)!},$$
$$\psi_k(t) = \int_{t_k}^{t_{k+1}} K^1(t, s) \exp\left(-\frac{t_{k+1} - s}{RC}\right) ds, \qquad (19)$$

*and the coefficients $[\mathbf{c}]_k = c_k$ and $[\mathbf{d}]_i = d_i$ satisfy the matrix equations*

$$(\mathbf{G} + n\lambda \mathbf{I})\mathbf{c} + \mathbf{F}\mathbf{d} = \mathbf{q},$$
$$\mathbf{F}'\mathbf{c} = \mathbf{0}, \qquad (20)$$

*with $[\mathbf{G}]_{kl} = \langle \psi_k, \psi_l \rangle$, $[\mathbf{F}]_{ki} = \langle \phi_k, \chi_i \rangle$, and $[\mathbf{q}]_k = q_k$, for all $k, l = 1, 2, \ldots, n$, and $i = 1, 2, \ldots, m$.*

*Proof.* Since the inner-product $\langle \phi_k, u \rangle$ describes the measurements performed by the LIF neuron with random thresholds described by (6), the minimizer of (17) is exactly the optimal estimate of $u$ encoded into the time sequence $(t_k)$, $k = 1, 2, \ldots, n$. The rest of the proof follows from Theorem 3 of Appendix A.3.

The representation functions $\psi_k$ are given by

$$\begin{aligned} \psi_k(t) &= \mathcal{P}_1 \phi_k = \langle \mathcal{P}_1 \phi_k, K_t \rangle \\ &= \langle \phi_k, \mathcal{P}_1 K_t \rangle = L_k K_t^1 \\ &= \int_{t_k}^{t_{k+1}} K^1(t, s) \exp\left(-\frac{t_{k+1} - s}{RC}\right) ds. \end{aligned} \qquad (21)$$

Finally, the entries of the matrices $\mathbf{F}$ and $\mathbf{G}$ are given by

$$[\mathbf{F}]_{ki} = \int_{t_k}^{t_{k+1}} \chi_i(s) \exp\left(-\frac{t_{k+1} - s}{RC}\right) ds,$$
$$[\mathbf{G}]_{kl} = \langle \psi_k, \psi_l \rangle = \int_{\mathcal{T}} \psi_k^{(m)}(s) \psi_l^{(m)}(s) \, ds, \qquad (22)$$

for all $k, l = 1, 2, \ldots, n$, and $i = 1, 2, \ldots, m$. The system of (20) is identical to (A.8) of Theorem 3 of Appendix A.3.     □

*Algorithm 1.* The coefficients **c** and **d** satisfying the system of (20) are given by

$$\mathbf{c} = \mathbf{M}^{-1}\left(\mathbf{I} - \mathbf{F}(\mathbf{F}'\mathbf{M}^{-1}\mathbf{F})^{-1}\mathbf{F}'\mathbf{M}^{-1}\right)\mathbf{q},$$

$$\mathbf{d} = (\mathbf{F}'\mathbf{M}^{-1}\mathbf{F})^{-1}\mathbf{F}'\mathbf{M}^{-1}\mathbf{q}, \tag{23}$$

with $\mathbf{M} = \mathbf{G} + n\lambda\mathbf{I}$.

*Proof.* The exact form of the coefficients above is derived as part of the results of Algorithm 6 (see Appendix A.3). The latter algorithm also shows how to evaluate the coefficients **c** and **d** based on the *QR* decomposition of the matrix **F**. □

*3.2. Recovery in $\mathcal{S}_1$ and $\mathcal{S}_2$.* In this section we provide detailed algorithms for reconstruction of stimuli in $\mathcal{S}_1$ and $\mathcal{S}_2$, respectively, encoded with LIF neurons with random thresholds. In the explicit form given, the algorithms can be readily implemented.

*3.2.1. Recovery of $\mathcal{S}_1$-Stimuli Encoded with a LIF Neuron with Random Threshold.* The stimuli $u$ in this section are elements of the Sobolev space $\mathcal{S}_1$. Thus, stimuli are modeled as absolutely continuous functions on $[0, 1]$ whose derivative can be defined in a weak sense. The Sobolev space $\mathcal{S}_1$ endowed with the inner-product

$$\langle u, v \rangle = u(0)v(0) + \int_0^1 u'(s)v'(s)\,ds \tag{24}$$

is a RKHS with reproducing kernel given by (see also (4))

$$K(t,s) = 1 + \int_0^1 1(s > \tau) \cdot 1(t > \tau)\,d\tau = 1 + \min(t,s). \tag{25}$$

The sampling functions $\phi_k(t)$, $k = 1, 2, \ldots, n$, given by (10), amount to

$$\frac{\phi_k(t)}{RC}$$

$$= 1 - \exp\left(-\frac{t_{k+1} - t_k}{RC}\right)$$

$$+ \left[1 - \exp\left(-\frac{t_{k+1} - t_k}{RC}\right)\right]t \cdot 1(t \le t_k)$$

$$+ \left[t - RC\exp\left(-\frac{t_{k+1} - t}{RC}\right) + (RC - t_k)\exp\left(-\frac{t_{k+1} - t_k}{RC}\right)\right]$$

$$\cdot 1(t_k < t \le t_{k+1})$$

$$+ \left[t_{k+1} - t_k\exp\left(-\frac{t_{k+1} - t_k}{RC}\right) - RC\left(1 - \exp\left(-\frac{t_{k+1} - t_k}{RC}\right)\right)\right]$$

$$\cdot 1(t_{k+1} < t). \tag{26}$$

The representation functions $\psi_k(t)$ are given, as before, by

$$\psi_k(t) = \langle \psi_k, K_t \rangle = \langle \phi_k, \mathcal{P}_1 K_t \rangle$$

$$= L_k K_t - L_k K_t^0 \tag{27}$$

$$= \phi_k(t) - RC\left(1 - \exp\left(-\frac{t_{k+1} - t_k}{RC}\right)\right),$$

for all $k = 1, 2, \ldots, n$. For the entries of **G** and **F** from (22) and (24) we have that

$$\frac{[\mathbf{G}]_{kl}}{(RC)^2} = \begin{cases} \left(1 - \exp\left(-\dfrac{t_{l+1} - t_l}{RC}\right)\right) \\ \quad \times \left(t_{k+1} - RC - (t_k - RC)\exp\left(-\dfrac{t_{k+1} - t_k}{RC}\right)\right), & l < k, \\[4pt] t_{k+1} - \dfrac{3RC}{2} - 2(t_k - RC)\exp\left(-\dfrac{t_{k+1} - t_k}{RC}\right) \\ \quad + \left(t_k - \dfrac{RC}{2}\right)\exp\left(-\dfrac{t_{k+1} - t_k}{RC/2}\right), & l = k, \\[4pt] \left(1 - \exp\left(-\dfrac{t_{k+1} - t_k}{RC}\right)\right) \\ \quad \times \left(t_{l+1} - RC - (t_l - RC)\exp\left(-\dfrac{t_{l+1} - t_l}{RC}\right)\right), & l > k, \end{cases}$$

$$[\mathbf{F}]_{k1} = RC\left(1 - \exp\left(-\frac{t_{k+1} - t_k}{RC}\right)\right), \tag{28}$$

for all $k = 1, 2, \ldots, n$, and all $l = 1, 2, \ldots, n$.

*Algorithm 2.* The minimizer $\hat{u} \in \mathcal{S}_1$ is given by (18) where

    (i) the coefficients **d** and **c** are given by (23) with the elements of the matrices **G** and **F** specified by (28) and,

    (ii) the representation functions $(\psi_k)$, $k = 1, 2, \ldots, n$, are given by (27) and (26).

*Remark 2.* If the $\mathcal{S}_1$-stimuli are encoded with an ideal IAF neuron with random threshold, the quantities of interest for implementing the reconstruction Algorithm 2 are given by

$$\phi_k(t) = \begin{cases} t_{k+1} - t_k + (t_{k+1} - t_k)t, & t \le t_k, \\[4pt] t_{k+1} - t_k - \dfrac{t^2}{2} + t_{k+1}t - \dfrac{t_k^2}{2}, & t_k < t \le t_{k+1}, \\[4pt] t_{k+1} - t_k + \dfrac{t_{k+1}^2 - t_k^2}{2}, & t_{k+1} < t, \end{cases}$$

$$\psi_k(t) = \phi_k(t) - (t_{k+1} - t_k),$$

$$[\mathbf{G}]_{kl} = \begin{cases} \dfrac{1}{2}\left(t_{l+1}^2 - t_l^2\right)(t_{k+1} - t_k), & l < k, \\[4pt] \dfrac{1}{3}(t_{k+1} - t_k)^2(t_{k+1} + 2t_k), & l = k, \\[4pt] \dfrac{1}{2}\left(t_{k+1}^2 - t_k^2\right)(t_{l+1} - t_l), & l > k, \end{cases} \tag{29}$$

$$[\mathbf{F}]_{k1} = t_{k+1} - t_k,$$

for all $k = 1, 2, \ldots, n$, and all $l = 1, 2, \ldots, n$. Note that the above quantities can also be obtained by taking the limits of (8), (26), (27), (28) when $R \to \infty$.

*3.2.2. Recovery of $\delta_2$-Stimuli Encoded with a LIF Neuron with Random Threshold.* In this section stimuli $u$ belong to the Sobolev space $\delta_2$, that is, the space of signals with absolutely continuous first-order derivatives. Endowed with the inner-product

$$\langle u, v \rangle = u(0)v(0) + u'(0)v'(0) + \int_0^1 u''(s)v''(s) \, ds, \quad (30)$$

$\delta_2$ is a RKHS with reproducing kernel

$$K(s, t) = 1 + ts + \int_0^{\min(s,t)} (s - \tau)(t - \tau) \, d\tau$$

$$= 1 + ts + \frac{1}{2} \min(s, t)^2 \max(s, t) - \frac{1}{6} \min(s, t)^3. \tag{31}$$

The sampling functions $\phi_k$, $k = 1, 2, \ldots, n$, are given by (10) and are equal to

$$e^{t_{k+1}/RC} \phi_k(t)$$

$$= g_k(t) + \left[ t^2 \frac{f_1(t_{k+1}) - f_1(t_k)}{2} - t^3 \frac{f_0(t_{k+1}) - f_0(t_k)}{6} \right]$$

$$\cdot 1(t \le t_k)$$

$$+ \left[ t^2 \frac{f_1(t_{k+1}) - f_1(t)}{2} - t^3 \frac{f_0(t_{k+1}) - f_0(t)}{6} \right.$$

$$\left. + t \frac{f_2(t) - f_2(t_k)}{2} - \frac{f_3(t) - f_3(t_k)}{6} \right] \tag{32}$$

$$\cdot 1(t_k < t \le t_{k+1})$$

$$+ \left[ t \frac{f_2(t_{k+1}) - f_2(t_k)}{2} - \frac{f_3(t_{k+1}) - f_3(t_k)}{6} \right]$$

$$\cdot 1(t_{k+1} < t),$$

where the functions $f_0, f_1, f_2, f_3 : \mathcal{T} \mapsto \mathbb{R}$ are of the form

$$f_0(x) = RC \exp\left(\frac{x}{RC}\right),$$

$$f_1(x) = RC(x - RC) \exp\left(\frac{x}{RC}\right),$$

$$f_2(x) = RC\left((RC)^2 + (x - RC)^2\right) \exp\left(\frac{x}{RC}\right),$$

$$f_3(x) = RC\left((x - RC)^3 + (RC)^2(3x - 5RC)\right) \exp\left(\frac{x}{RC}\right),$$

$$g_k(t) = f_0(t_{k+1}) - f_0(t_k) + t(f_1(t_{k+1}) - f_1(t_k)). \tag{33}$$

Note that for each $i$, $i = 0, 1, 2, 3$,

$$f_i(x) = \int_0^1 x^i \exp\left(\frac{x}{RC}\right) \, dx. \tag{34}$$

The representation functions are equal to

$$\psi_k(t) = \phi_k(t) - e^{-t_{k+1}/RC} g_k(t), \tag{35}$$

and the entries of $\mathbf{F}$ are given by

$$[\mathbf{F}]_{k1} = e^{-t_{k+1}/RC}(f_0(t_{k+1}) - f_0(t_k)),$$
$$\tag{36}$$
$$[\mathbf{F}]_{k2} = e^{-t_{k+1}/RC}(f_1(t_{k+1}) - f_1(t_k)).$$

Finally, the entries of $\mathbf{G}$ can also be computed in closed form. To evaluate them note that $\psi_k(0) = \psi_k'(0) = 0$, for all $k$, $k = 1, 2, \ldots, n$. Therefore

$$[\mathbf{G}]_{kl} = \langle \psi_k, \psi_l \rangle = \int_0^1 \psi_k''(s)\psi_l''(s) \, ds,$$

$$\frac{\psi_k''(t)}{RC}$$

$$= \begin{cases} t_{k+1} - RC - (t_k - RC) \exp\left(-\dfrac{t_{k+1} - t_k}{RC}\right) \\ \quad -t\left(1 - \exp\left(-\dfrac{t_{k+1} - t_k}{RC}\right)\right), & t \le t_k, \\[2mm] t_{k+1} - t - RC\left(1 - \exp\left(-\dfrac{t_{k+1} - t}{RC}\right)\right), & t_k < t \le t_{k+1}, \\[2mm] 0, & t_{k+1} < t. \end{cases}$$

$$\tag{37}$$

Denoting by

$$y_k = 1 - \exp\left(-\frac{t_{k+1} - t_k}{RC}\right),$$
$$\tag{38}$$
$$z_k = t_{k+1} - RC - (t_k - RC) \exp\left(-\frac{t_{k+1} - t_k}{RC}\right),$$

the entries of the $\mathbf{G}$ matrix amount to

$$[\mathbf{G}]_{kl}$$

$$= \left(\frac{1}{3} t_k^3 y_k y_l - \frac{1}{2} t_k^2 (y_k z_l + y_l z_k) + t_k z_k z_l \right.$$

$$+ z_k \left((t_{k+1} - RC)(t_{k+1} - t_k) - \frac{t_{k+1}^2 - t_k^2}{2} + (RC)^2 y_k\right)$$

$$\left. + y_k\left(\frac{1}{2}(t_{k+1} - RC)\left(t_{k+1}^2 - t_k^2\right) - \frac{1}{3}\left(t_{k+1}^3 - t_k^3\right) + (RC)^2 z_k\right)\right)$$

$$\cdot 1(k < l)$$

$$+ \left( \frac{1}{3}t_k^3 y_k^2 - t_k^2 y_k z_k + t_k z_k^2 + \frac{1}{3}(t_{k+1} - t_k)^3 \right.$$

$$- RC(t_{k+1} - t_k)^2 - 2(RC)^2(t_{k+1} - t_k)(1 - 2y_k)$$

$$\left. + \frac{1}{2}(RC)^3 \left( 1 - \exp\left( -\frac{t_{k+1} - t_k}{RC/2} \right) \right) \right)$$

$$\cdot \mathbf{1}(k = l)$$

$$+ \left( \frac{1}{3}t_l^3 y_l y_k - \frac{1}{2}t_l^2 (y_l z_k + y_k z_l) + t_l z_l z_k \right.$$

$$+ z_l \left( (t_{l+1} - RC)(t_{l+1} - t_l) - \frac{t_{l+1}^2 - t_l^2}{2} + (RC)^2 y_l \right)$$

$$\left. + y_l \left( \frac{1}{2}(t_{l+1} - RC)\left( t_{l+1}^2 - t_l^2 \right) - \frac{1}{3}\left( t_{l+1}^3 - t_l^3 \right) + (RC)^2 z_l \right) \right)$$

$$\cdot \mathbf{1}(k > l). \tag{39}$$

*Algorithm 3.* The minimizer $\hat{u} \in \mathscr{S}_2$ is given by (18) where

(i) the coefficients $\mathbf{d}$ and $\mathbf{c}$ are given by (23) with the elements of the matrices $\mathbf{G}$ and $\mathbf{F}$ specified by (39) and (36), respectively, and,

(ii) the representation functions $(\psi_k)$, $k = 1, 2, \ldots, n$, are given by (35) and (32).

*Remark 3.* If $\mathscr{S}_2$-stimuli are encoded with an ideal IAF neuron with random threshold, the quantities of interest in implementing the reconstruction **Algorithm 3** are given by

$$\phi_k(t) = \psi_k(t) + t_{k+1} - t_k + \frac{t(t_{k+1}^2 - t_k^2)}{2},$$

$$\psi_k(t) = \begin{cases} \dfrac{t^2}{4}\left( t_{k+1}^2 - t_k^2 \right) - \dfrac{t^3}{6}(t_{k+1} - t_k), & t \le t_k, \\[2mm] \dfrac{t_k^4}{24} - \dfrac{t}{6}t_k^3 + \dfrac{t^2}{4}t_{k+1}^2 - \dfrac{t^3}{6}t_{k+1} + \dfrac{t^4}{24}, & t_k < t \le t_{k+1}, \\[2mm] -\dfrac{1}{24}\left( t_{k+1}^4 - t_k^4 \right) + \dfrac{t}{6}\left( t_{k+1}^3 - t_k^3 \right), & t_{k+1} < t, \end{cases}$$

$$[\mathbf{G}]_{kl} = \begin{cases} \dfrac{\left( t_{l+1}^3 - t_l^3 \right)\left( t_{k+1}^2 - t_k^2 \right)}{12} - \dfrac{\left( t_{l+1}^4 - t_l^4 \right)(t_{k+1} - t_k)}{24}, & l < k, \\[2mm] \dfrac{1}{4}(t_{k+1} - t_k)^2 \left( \dfrac{1}{3}t_k^3 + t_k t_{k+1}^2 + \dfrac{1}{5}(t_{k+1} - t_k)^3 \right), & l = k, \\[2mm] \dfrac{\left( t_{k+1}^3 - t_k^3 \right)\left( t_{l+1}^2 - t_l^2 \right)}{12} - \dfrac{\left( t_{k+1}^4 - t_k^4 \right)(t_{l+1} - t_l)}{24}, & l > k, \end{cases}$$

$$[\mathbf{F}]_{ki} = \frac{t_{k+1}^i - t_k^i}{i}, \tag{40}$$

for all $k = 1, 2, \ldots, n$, all $l = 1, 2, \ldots, n$, and all $i = 1, 2$. Note that the above quantities can also be obtained by taking the limits of (8), (32), (35), (36), (39) when $R \to \infty$.

### 3.3. Examples.

In this section we present two examples that demonstrate the performance of the stimulus reconstruction algorithms presented above. In the first example, a simplified model of the temporal contrast derived from the photocurrent drives the spiking behavior of a LIF neuron with random threshold. While the effective bandwidth of the temporal contrast is typically unknown, the analog waveform is absolutely continuous and the first-order derivative can be safely assumed to be absolutely continuous as well.

In the second example, the stimulus is encoded by a pair of nonlinear rectifier circuits each cascaded with a LIF neuron. The rectifier circuits separate the positive and the negative components of the stimulus. Both signal components are assumed to be absolutely continuous. However, the first-order derivatives of the component signals are no longer absolutely continuous.

In both cases the encoding circuits are of specific interest to computational neuroscience and neuromorphic engineering. We argue that Sobolev spaces are a natural choice for characterizing the stimuli that are of interest in these applications and show that the algorithms perform well and can essentially recover the stimulus in the presence of noise.

### 3.3.1. Encoding of Temporal Contrast with a LIF Neuron.

A key signal in the visual system is the (positive) input photocurrent. Nonlinear circuits of nonspiking neurons in the retina extract the temporal contrast of the visual field from the photocurrent. The temporal contrast is then presented to the first level of spiking neurons, that is, the retinal ganglion cells (RGCs) [17]. If $I = I(t)$ is the input photocurrent, then a simplified model for the temporal contrast $u = u(t)$ is given by the equation

$$u(t) = \frac{d \log(I(t))}{dt} = \frac{1}{I(t)}\frac{dI}{dt}. \tag{41}$$

This model has been employed in the context of address event representation (AER) circuits for silicon retina and related hardware applications [18]. It is aboundingly clear that even when the input bandwidth of the photocurrent $I$ is known, the efficient bandwidth of the actual input $u$ to the neuron cannot be analytically evaluated. However, the somatic input is still a continuously differentiable function, and it is natural to assume that it belongs to the Sobolev spaces $\mathscr{S}_1$ and $\mathscr{S}_2$. LIF neuron models have been used to fit responses of RGCs neurons in the early visual system [19].

In our example the input photocurrent is assumed to be a positive bandlimited function with bandwidth $\Omega = 2\pi \cdot 30$ rads/s. The neuron is modeled as a LIF neuron with random threshold. After each spike, the value of the neuron threshold was picked from a Gaussian distribution $\mathcal{N}(\delta, \sigma^2)$. The LIF neuron parameters were $b = 2.5$, $\delta = 2.5$, $\sigma = 0.1$, $C = 0.01$, and $R = 40$ (all nominal values). The neuron fired a total of 108 spikes.

Figure 2(a) shows the optimal recovery in $\mathscr{S}_2$ with regularization parameter $\lambda = 1.3 \times 10^{-14}$. Figure 2(b) shows the Signal-to-Noise Ratio for various values of the smoothing parameter $\lambda$ in $\mathscr{S}_1$ (blue line) and $\mathscr{S}_2$ (green line). The red
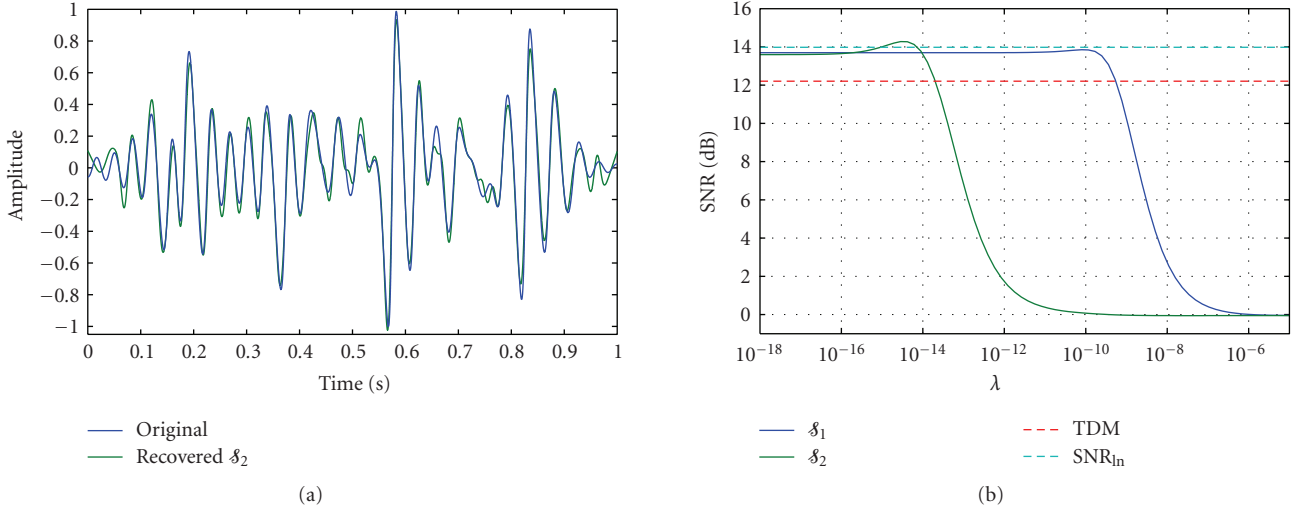
FIGURE 2: Recovery of temporal contrast encoded with a LIF. The stimulus and its first-order derivative are absolutely continuous.

line shows the SNR when the perfect recovery algorithm of [1] with the sinc kernel $K(s,t) = \sin(2\Omega(t-s))/\pi(t-s)$, $(s,t) \in \mathbb{R}^2$, is used (other choices of sinc kernel bandwidth give similar or lower SNR). The cyan line represents the threshold SNR defined as $10\log_{10}(\delta/\sigma)$. Recovery in $\mathcal{S}_2$ outperforms recovery in $\mathcal{S}_1$ but gives satisfactory results for a smaller range of the smoothing parameter. For a range of the regularization parameter $\lambda$ both reconstructions outperform the performance of the recovery algorithm for bandlimited stimuli based upon the sinc kernel [1]. Finally, the stimulus recovery SNR is close to the threshold SNR.

*3.3.2. Encoding the Stimulus Velocity with a Pair of LIF Neurons.* The stimulus is encoded by a pair of nonlinear rectifier circuits each cascaded with a LIF neuron. The rectifier circuits separate the positive and the negative components of the stimulus. (see Figure 3). Such a clipping-based encoding mechanism has been used for modeling the direction selectivity of the H1 cell in the fly lobula plate [7].

Formally, the stimulus is decomposed into its positive $u_+$ and negative $u_-$ components by the nonlinear clipping mechanism:

$$u_+(t) = \max(u(t), 0),$$
$$u_-(t) = -\min(u(t), 0), \qquad (42)$$
$$u(t) = u_+(t) - u_-(t).$$

As an example, the input stimulus $u$ is a bandlimited function with bandwidth $\Omega = 2\pi \cdot 30$ rad/s. After clipping, each signal component is no longer a bandlimited or a differentiable function. However it is still an absolutely continuous function and, therefore, an element of the Sobolev space $\mathcal{S}_1$. Each component is encoded with two identical LIF neurons with parameters $b = 1.6$, $\delta = 1$, $R = 40$, and $C = 0.01$ (all nominal values). The thresholds of the two neurons are deterministic, that is, there is no noise in the encoding circuit. Each neuron produced 180 spikes.

By applying the recovery algorithm for $\mathcal{S}_1$-signals, the two signal components are separately recovered. Finally, by subtracting the recovered signal components, the original stimulus is reconstructed. Figure 4 shows the recovered version of the positive and negative signal components and of the original stimulus. As it can be seen, both components are very accurately recovered. Note that since the threshold is deterministic, the regularization (or smoothing) parameter $\lambda$ is set to 0. The corresponding SNRs for the positive component, negative component, and original stimulus were 27.3 dB, 27.7 dB and 34 dB, respectively.

## 4. Reconstruction of Stimuli Encoded with a Population of LIF Neurons with Random Thresholds

In this section we encode stimuli with a population of leaky integrate-and-fire neurons with random thresholds. As in Section 3, the stimuli are assumed to be elements of a Sobolev space. We first derive the general reconstruction algorithm. We then work out the reconstruction of stimuli that are absolutely continuous and stimuli that have an absolutely continuous first-order derivative. Examples of the reconstruction algorithm are given at the end of this section.

*4.1. Reconstruction of Stimuli in Sobolev Spaces.* Let $u = u(t)$, $t \in \mathcal{T}$, be a stimulus in the Sobolev space $\mathcal{S}_m$, $m \in \mathbb{N}^*$. An optimal estimate of $\hat{u}$ of $u$ is obtained by minimizing the cost functional

$$\frac{1}{n}\sum_{j=1}^{N}\sum_{k=1}^{n_j}\left(\frac{q_k^j - \langle \phi_k^j, u \rangle}{C^j \sigma^j}\right)^2 + \lambda \|\mathcal{P}_1 u\|^2, \qquad (43)$$

where $n = \sum_{j=1}^{N} n_j$ and $\mathcal{P}_1 : \mathcal{S}_m \mapsto \mathcal{H}_1$ is the projection of the Sobolev space $\mathcal{S}_m$ to $\mathcal{H}_1$. In what follows $\mathbf{q}$ denotes the column vector $\mathbf{q} = [(1/(C^1 \sigma^1))\mathbf{q}^1; \ldots; (1/(C^N \sigma^N))\mathbf{q}^N]$ with $[\mathbf{q}^j]_k = q_k^j$, for all $j = 1, 2, \ldots, N$, and all $k = 1, 2, \ldots, n_j$. We have the following result.
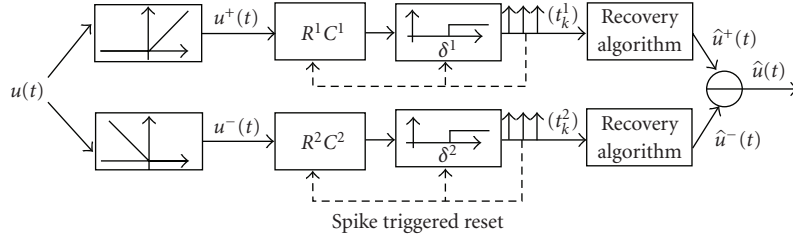
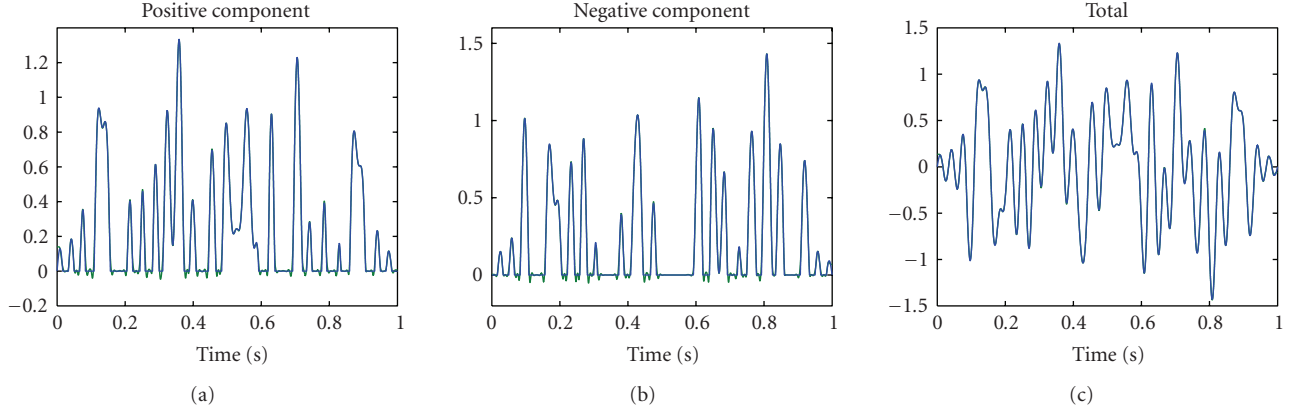FIGURE 3: Circuit for encoding of stimuli velocity.



FIGURE 4: Encoding the stimulus velocity with a pair of rectifier LIF Neurons. (a) Positive signal component. (b) Negative signal component. (c) Reconstructed stimulus.

**Theorem 2.** *Assume that the stimulus $u = u(t)$, $t \in [0,1]$ is encoded into a time sequence $(t_k^j)$, $j = 1,2,\ldots,N$, $k = 1,2,\ldots,n_j$, with a population of LIF neurons with random thresholds that is fully described by* (13). *The optimal estimate $\hat{u}$ of $u$ is given by*

$$\hat{u} = \sum_{i=1}^{m} d_i \chi_i + \sum_{j=1}^{N} \frac{1}{C^j \sigma^j} \sum_{k=1}^{n_j} c_k^j \psi_k^j, \tag{44}$$

*where*

$$\chi_i(t) = \frac{t^{i-1}}{(i-1)!},$$
$$\psi_k^j(t) = \int_{t_k^j}^{t_{k+1}^j} K^1(t,s) \exp\left(-\frac{t_{k+1}^j - s}{R^j C^j}\right) ds. \tag{45}$$

*The coefficients vectors $\mathbf{c} = [\mathbf{c}^1;\ldots;\mathbf{c}^N]$ with $[\mathbf{c}^j]_k = c_k^j$, for all $j = 1,2,\ldots,N$, and all $k = 1,2,\ldots,n_j$, and $[\mathbf{d}]_i = d_i$, for all $i = 1,2,\ldots,m$, satisfy the matrix equations*

$$\left(\mathbf{G} + \lambda \sum_{j=1}^{N} n_j \cdot \mathbf{I}\right)\mathbf{c} + \mathbf{F}\mathbf{d} = \mathbf{q},$$
$$\mathbf{F}'\mathbf{c} = \mathbf{0}, \tag{46}$$

*where $\mathbf{G}$ is a block square matrix defined as*

$$\mathbf{G} = \begin{bmatrix} \frac{1}{(C^1\sigma^1)^2}\mathbf{G^{11}} & \cdots & \frac{1}{C^1\sigma^1 C^N\sigma^N}\mathbf{G^{1N}} \\ \vdots & \ddots & \vdots \\ \frac{1}{C^N\sigma^N C^1\sigma^1}\mathbf{G^{N1}} & \cdots & \frac{1}{(C^N\sigma^N)^2}\mathbf{G^{NN}} \end{bmatrix}, \tag{47}$$

*with $[\mathbf{G}^{ij}]_{kl} = \langle \psi_k^i, \psi_l^j \rangle$, for all $i, j = 1,\ldots,N$, all $k = 1,\ldots,n_i$, and all $l = 1,\ldots,n_j$. Finally, $\mathbf{F}$ is a block matrix defined as $\mathbf{F} = [(1/(C^1\sigma^1))\mathbf{F}^1;\ldots;(1/(C^N\sigma^N))\mathbf{F}^N]$ with $[\mathbf{F}^j]_{ki} = \langle \phi_k^j, \chi_i \rangle$, for all $j = 1,2,\ldots,N$, all $k = 1,2,\ldots,n_j$, and all $i = 1,2,\ldots,m$.*

*Proof.* The noise terms

$$q_k^j - \langle \phi_k^j, u \rangle \tag{48}$$

that appear in the cost functional (43) are independent Gaussian random variables with zero mean and variance $(C^j\sigma^j)^2$. Therefore, by normalizing the $t$-transform of each neuron with the noise standard deviation $C^j\sigma^j$, these random variables become i.i.d. with unit variance. After normalization, the linear functionals in (8) can be written as

$$L_k^j u = \int_{t_k^j}^{t_{k+1}^j} \frac{1}{C^j\sigma^j} u(s) \exp\left(-\frac{t_{k+1}^j - s}{R^j C^j}\right) ds. \tag{49}$$

This normalization causes a normalization in the sampling and reconstruction functions $\phi_k^j$ and $\psi_k^j$ as well as in the

entries of **F**. We have

$$\left[\mathbf{F}^j\right]_{ki} = \frac{1}{C^j \sigma^j} \int_{t_k^j}^{t_{k+1}^j} \chi_i(s) \exp\left(-\frac{t_{k+1}^j - s}{R^j C^j}\right) ds, \qquad (50)$$

for all $i = 1, 2, \ldots, m$, all $k = 1, 2, \ldots, n_j$, and all $j = 1, 2, \ldots, N$. The rest of the proof follows from Theorem 3. $\qquad \square$

*4.2. Recovery in $\mathcal{S}_1$ and $\mathcal{S}_2$.* In this section we provide detailed algorithms for reconstruction of stimuli in $\mathcal{S}_1$ and $\mathcal{S}_2$, respectively, encoded with a population of LIF neurons with random thresholds. As in Section 3.2, the algorithms provided can be readily implemented.

*4.2.1. Recovery of $\mathcal{S}_1$-Stimuli Encoded with a Population of LIF Neurons with Random Thresholds.* Let $u$ be an absolutely continuous signal in $\mathcal{T}$, that is, $u \in \mathcal{S}_1$. We have the following.

*Algorithm 4.* The minimizer $\hat{u} \in \mathcal{S}_1$ is given by (44) and

(i) the coefficients **d** and **c** are given by (23) with the elements of the matrices **G** and **F** specified in Theorem 2 and,

(ii) the representation functions $(\psi_k^j)$, $k = 1, 2, \ldots, n_j$, and $j = 1, 2, \ldots, N$, are essentially given by (27) and (26) (plus an added superscript $j$).

*Remark 4.* If $\mathcal{S}_1$-stimuli are encoded with a population of ideal IAF neurons with random thresholds, then the entries of the matrix **G** can be computed analytically. We have

$$\left[\mathbf{G}^{ij}\right]_{kl}$$
$$= \left[\frac{1}{2}\left(\tau_{l+1}^2 - \tau_l^2\right)(\tau_{k+1} - \tau_k)\right] \cdot 1(\tau_{l+1} < \tau_k)$$
$$+ \left[\frac{1}{2}\left(\left(\tau_k^2 - \tau_l^2\right)(\tau_{k+1} - \tau_k) + \left(\tau_{l+1}^2 - \tau_k^2\right)(\tau_{k+1} - \tau_{l+1})\right)\right.$$
$$\left. + \frac{1}{3}\left(\tau_{l+1}^3 - \tau_k^3\right) - \tau_k^2(\tau_{l+1} - \tau_k)\right]$$
$$\cdot 1(\tau_l \le \tau_k \le \tau_{l+1} \le \tau_{k+1})$$
$$+ \left[-\frac{1}{6}\left(\tau_{k+1}^3 - \tau_k^3\right) + \frac{1}{2}\tau_{l+1}\left(\tau_{k+1}^2 - \tau_k^2\right) - \frac{1}{2}\tau_l^2(\tau_{k+1} - \tau_k)\right]$$
$$\cdot 1(\tau_l \le \tau_k < \tau_{k+1} \le \tau_{l+1})$$
$$+ \left[-\frac{1}{6}\left(\tau_{l+1}^3 - \tau_l^3\right) + \frac{1}{2}\tau_{k+1}\left(\tau_{l+1}^2 - \tau_l^2\right) - \frac{1}{2}\tau_k^2(\tau_{l+1} - \tau_l)\right]$$
$$\cdot 1(\tau_k \le \tau_l < \tau_{l+1} \le \tau_{k+1})$$
$$+ \left[\frac{1}{2}\left(\left(\tau_l^2 - \tau_k^2\right)(\tau_{l+1} - \tau_l) + \left(\tau_{k+1}^2 - \tau_l^2\right)(\tau_{l+1} - \tau_{k+1})\right)\right.$$
$$\left. + \frac{1}{3}\left(\tau_{k+1}^3 - \tau_l^3\right) - \tau_l^2(\tau_{k+1} - \tau_l)\right]$$
$$\cdot 1(\tau_k \le \tau_l \le \tau_{k+1} \le \tau_{l+1})$$
$$+ \left[\frac{1}{2}\left(\tau_{k+1}^2 - \tau_k^2\right)(\tau_{l+1} - \tau_l)\right] \cdot 1(\tau_{k+1} < \tau_l),$$
$$(51)$$

Table 1: Nominal values of the neuron parameters ($\delta$ represents the mean value of the threshold value).

| Neuron | 1 | 2 | 3 | 4 |
|---|---|---|---|---|
| $b$ | 0.92 | 0.79 | 1.15 | 1.19 |
| $\delta$ | 2.94 | 2.61 | 2.76 | 2.91 |
| $R$ | 31.9 | 25.2 | 32.1 | 34.2 |
| $C$ | 0.01 | 0.01 | 0.01 | 0.01 |

where $\tau_k = t_k^i$, $\tau_{k+1} = t_{k+1}^i$, $\tau_l = t_l^j$, $\tau_{l+1} = t_{l+1}^j$, for all $i, j = 1, \ldots, N$, all $k = 1, \ldots, n_i$, and all $l = 1, \ldots, n_j$. The analytical evaluation of the entries of the matrix **F** is straightforward.

*4.2.2. Recovery of $\mathcal{S}_2$-Stimuli Encoded with a Population of LIF Neurons with Random Thresholds.* Let $u$ be a signal with absolutely continuous first-order derivative in $\mathcal{T}$, that is, $u \in \mathcal{S}_2$. We have the following.

*Algorithm 5.* The minimizer $\hat{u} \in \mathcal{S}_2$ is given by (44) and

(i) the coefficients **d** and **c** are given by (23) with the elements of the matrices **G** and **F** specified in Theorem 2 and,

(ii) the representation functions $(\psi_k^j)$, $k = 1, 2, \ldots, n_j$, and $j = 1, 2, \ldots, N$, are essentially given by (35) and (32) (plus an added superscript $j$).

*4.3. Examples.* In this section we present two examples that demonstrate the performance of the reconstruction algorithms for stimuli encoded with a population of neurons as presented above. In both cases the encoding circuits are of specific interest to neuromorphic engineering and computational neuroscience. The first example presented in Section 4.3.1 shows the results of recovery of the temporal contrast encoded with a population of LIF neurons with random thresholds. Note that in this example the stimulus is in $\mathcal{S}_2$ and therefore also in $\mathcal{S}_1$. Stimulus reconstruction as a function of threshold variability and the smoothing parameter are demonstrated. In the example in Section 4.3.2, the stimulus is encoded using, as in Section 3.3.2, a rectifier circuit and a population of neurons. Here the recovery can be obtained in $\mathcal{S}_1$ only. As expected, recovery improves as the size of the population grows larger.

*4.3.1. Encoding of Temporal Contrast with a Population of LIF Neurons.* We examine the encoding of the temporal contrast with a population of LIF neurons. In particular, the temporal contrast input $u$ was fed into a population of 4 LIF neurons with nominal parameters given in Table 1.

In each simulation, each neuron had a random threshold with standard deviation $\sigma^j$ for all $j = 1, 2, 3, 4$. Simulations were run for multiple values of $\delta^j/\sigma^j$ in the range $[5, 100]$, and the recovered versions were computed in both $\mathcal{S}_1$ and $\mathcal{S}_2$ spaces for multiple values of the smoothing parameter $\lambda$. Figure 5 shows the SNR of the recovered stimuli in $\mathcal{S}_1$ and $\mathcal{S}_2$.
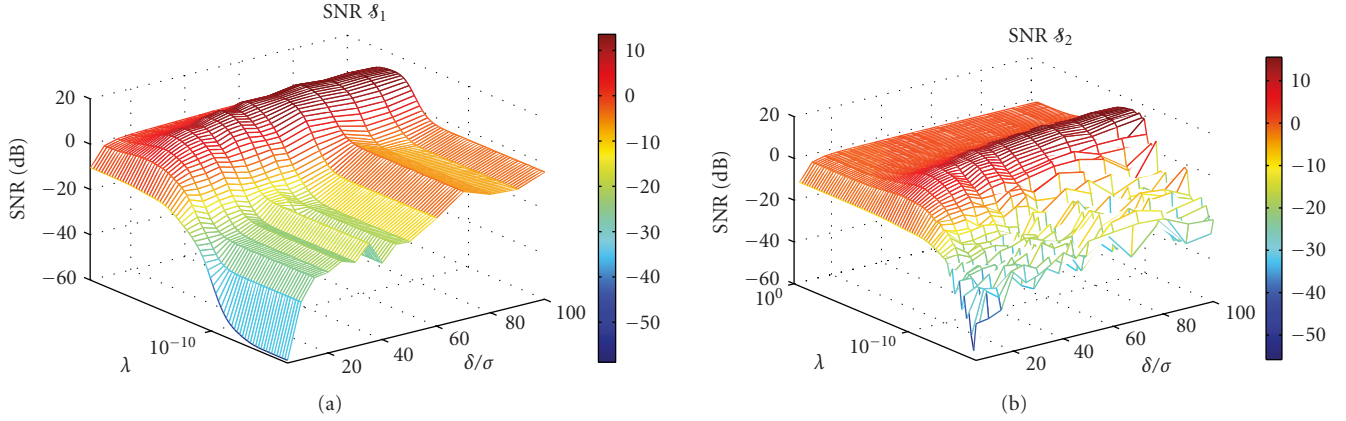
FIGURE 5: Signal-to-Noise Ratio for different noise threshold levels and different values of the smoothing parameter $\lambda$. The $x$-axis represents the threshold-to-noise ratio $\delta/\sigma$. (a) SNR for recovery in $\mathcal{S}_1$. (b) SNR for recovery in $\mathcal{S}_2$.
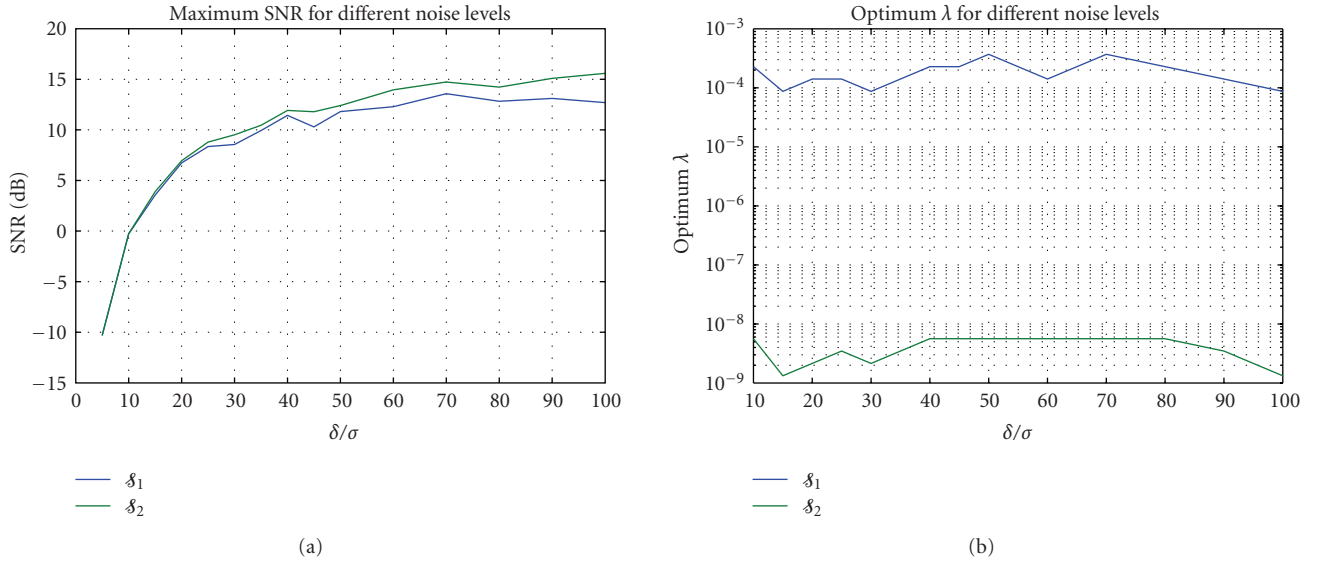


FIGURE 6: (a) Maximum SNR over all possible values of the smoothing parameter $\lambda$ for a fixed noise level $\delta/\sigma$. (b) Optimal value of the parameter $\lambda$ for which the recovered stimuli attain the maximum SNR. Blue line for $\mathcal{S}_1$ and green line for $\mathcal{S}_2$.

Figure 6 examines how the maximum SNR and the optimal value for the smoothing parameter that attains this maximum depend on the noise level. From Figures 5 and 6 we note that the

(i) recovery in $\mathcal{S}_2$ gives in general better results than recovery in $\mathcal{S}_1$. This is expected since $u \in \mathcal{S}_2 \subset \mathcal{S}_1$;

(ii) the optimal value of the smoothing parameter is largely independent of the noise level. This is due to the averaging in the cost functional across the population of neurons;

(iii) The encoding mechanism is very sensitive to the variability of the random threshold. In general if the threshold-to-noise ratio $\delta/\sigma$ is below 15, then accurate recovery is not possible (SNR < 5 dB).

### 4.3.2. Velocity Encoding with a Population of Rectifier LIF Neurons.

This example is a continuation of the example presented in Section 3.3.2. The positive and negative components of the stimulus are each fed into a population of 8 LIF neurons with random thresholds. The nominal values of the neuron parameters and the number of spikes that each neuron fired are given in Table 2. Using the same stimulus, the simulation was repeated one hundred times. In Figure 7 an example of the recovered positive and negative clipped signal components are shown each encoded with 1, 2, 4, and 8 neurons. The clipped signal components are elements of the Sobolev space $\mathcal{S}_1$ but not $\mathcal{S}_2$. The difference between the recovered components approximates the original stimulus (third column). The three columns correspond to the recovery of the positive and of the negative

TABLE 2: Nominal values of the neuron parameters and the number of spikes fired. For each neuron we also had $C_+^i = C_-^i = 0.01$ and $\sigma_+^i = \delta_+^i/20$ and $\sigma_-^i = \delta_-^i/20$ for all $i = 1, 2, \ldots, 8$.

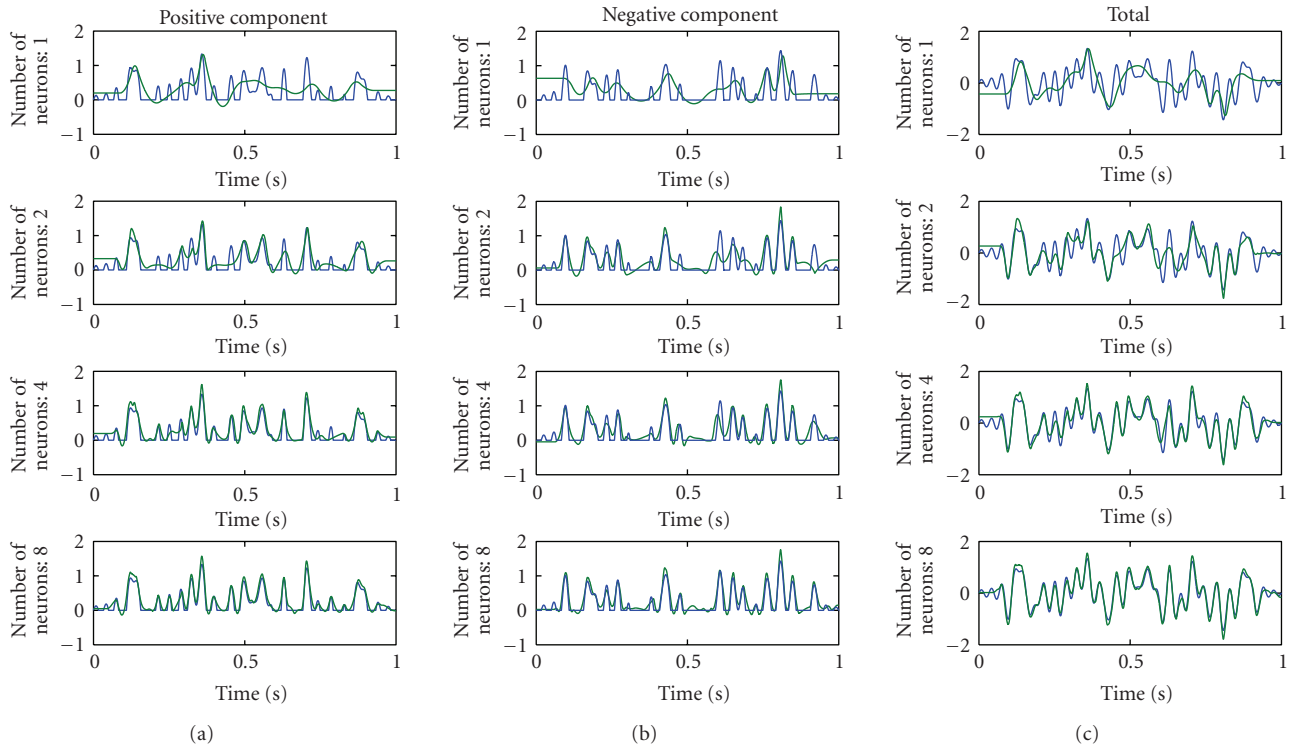| Neuron | 1 | 2 | 3 | 4 | 5 | 6 | 7 | 8 |
|---|---|---|---|---|---|---|---|---|
| $b_+$ | 0.14 | 0.25 | 0.15 | 0.28 | 0.15 | 0.25 | 0.14 | 0.16 |
| $b_-$ | 0.12 | 0.22 | 0.24 | 0.21 | 0.19 | 0.23 | 0.23 | 0.24 |
| $\delta_+$ | 2.03 | 2.35 | 1.61 | 2.11 | 1.64 | 1.52 | 2.01 | 1.85 |
| $\delta_-$ | 1.86 | 2.1 | 2.18 | 1.75 | 2.06 | 1.81 | 2.24 | 2.23 |
| $R_+$ | 35 | 42 | 42 | 41 | 47 | 35 | 26 | 32 |
| $R_-$ | 49 | 43 | 40 | 43 | 41 | 43 | 41 | 44 |
| Spikes+ | 19 | 22 | 25 | 26 | 25 | 35 | 19 | 22 |
| Spikes− | 19 | 23 | 22 | 26 | 21 | 27 | 21 | 22 |



FIGURE 7: Recovery of absolutely continuous stimuli encoded with a population of LIF neurons with random thresholds.

components, and the total stimulus, respectively. The four rows show the recovery when 1, 2, 4, and 8 encoding neurons are, respectively, used. Blue lines correspond to the original stimuli and green to the recovered ones. It can be seen that the recovery improves when more neurons are used. This can also be seen from Figure 8 where the corresponding mean value SNRs are plotted. The error bars in the same figure correspond to the standard deviation of the associated SNR.

## 5. Conclusions

In this paper we presented a general approach to the reconstruction of sensory stimuli encoded with LIF neurons with random thresholds. We worked out in detail the reconstruction of stimuli modeled as elements of Sobolev spaces with absolutely continuous, and with absolutely continuous first-order derivatives. Clearly the approach advocated here is rather general, and the same formalism can be applied to other Sobolev spaces or other RKHSs. Finally, we note that the recovery methodology employed here also applies to stimuli encoded with a population of LIF neurons.

We extensively discussed the stimulus reconstruction results for Sobolev spaces and gave detailed examples in the hope that practicing systems neuroscientists will find them easy to apply or will readily adapt them to other models of sensory stimuli and thus to other RKHSs of interest. The work presented here can also be applied to statistical learning in neuroscience. This and other closely related topics will be presented elsewhere.
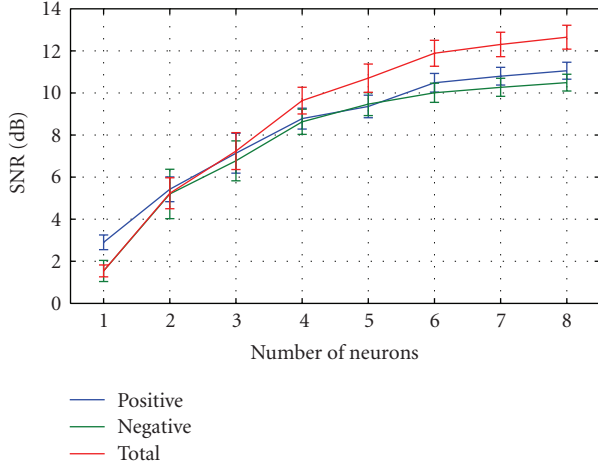
FIGURE 8: SNR for the positive (blue), negative (green), and total stimulus (red) as a function of the number of encoding neurons.

# Appendix

## A. Theory of RKHS

*A.1. Elements of Reproducing Kernel Hilbert Spaces.*

*Definition 1.* A Hilbert space $\mathcal{H}$ of functions defined on a domain $\mathcal{T}$ associated with the inner-product $\langle\cdot,\cdot\rangle : \mathcal{H} \times \mathcal{H} \mapsto \mathbb{R}$ is called a Reproducing Kernel Hilbert Space (RKHS) if for each $t \in \mathcal{T}$ the evaluation functional $E_t : \mathcal{H} \mapsto \mathbb{R}$ with $E_t u = u(t)$, $u \in \mathcal{H}$, $t \in \mathcal{T}$, is a bounded linear functional.

From the Riesz representation theorem (see Section A.2), for every $t \in \mathcal{T}$ and every $u \in \mathcal{H}$ there exists a function $K_t \in \mathcal{H}$ such that

$$\langle K_t, u \rangle = u(t). \tag{A.1}$$

The above equality is known as the reproducing property [15].

*Definition 2.* A function $K : \mathcal{T} \times \mathcal{T} \mapsto \mathbb{R}$ is a reproducing kernel of the RKHS $\mathcal{H}$ if and only if

(1) $K(\cdot, t) \in \mathcal{H}$, for all $t \in \mathcal{T}$,

(2) $\langle u, K(\cdot, t) \rangle = u(t)$, for all $t \in \mathcal{T}$ and $u \in \mathcal{H}$.

From the above definition it is clear that $K(s, t) = \langle K(\cdot, s), K(\cdot, t) \rangle$. Moreover, it is easy to show that every RKHS has a unique reproducing kernel [15].

*A.2. Riesz Representation Theorem.* Here we state the Riesz Lemma, also known as the Riesz Representation Theorem.

**Lemma 3.** *Let $\mathcal{H}$ be a Hilbert space and let $L : \mathcal{H} \mapsto \mathbb{R}$ be a continuous (bounded) linear functional. Then there exists a unique element $v \in \mathcal{H}$ such that*

$$Lu = \langle v, u \rangle, \tag{A.2}$$

*for all $u \in \mathcal{H}$.*

*Proof.* The proof can be found in [20]. Note that if $\mathcal{H}$ is a RKHS with reproducing kernel $K$, then the unique element can be easily found since

$$v(t) = \langle v, K_t \rangle = LK_t. \tag{A.3}$$
$\square$

*A.3. Smoothing Splines in Sobolev Spaces.* Suppose that a receiver reads the following measurements

$$q_k = \langle \phi_k, u \rangle + \varepsilon_k, \tag{A.4}$$

where $\phi_k \in \mathcal{S}_m$ and $\varepsilon_i$ are i.i.d. gaussian random variables, with zero mean and variance 1, for all $k = 1, 2, \ldots, n$. An optimal estimate $\hat{u}$ of $u$ minimizes the cost functional

$$\frac{1}{n} \sum_{k=1}^{n} (q_k - \langle \phi_k, u \rangle)^2 + \lambda \|\mathcal{P}_1 u\|^2, \tag{A.5}$$

where $\mathcal{P}_1 : \mathcal{S}_m \mapsto \mathcal{H}_1$ is the projection of the Sobolev space $\mathcal{S}_m$ to $\mathcal{H}_1$. Intuitively, the nonnegative parameter $\lambda$ regulates the choice of the estimate $\hat{u}$ between faithfulness to data fitting ($\lambda$ small) and maximum smoothness of the recovered signal ($\lambda$ large). We have the following theorem.

**Theorem 3.** *The minimizer $\hat{u}$ of* (A.5) *is given by*

$$\hat{u} = \sum_{i=1}^{m} d_i \chi_i + \sum_{k=1}^{n} c_k \psi_k, \tag{A.6}$$

*where*

$$\chi_i(t) = \frac{t^{i-1}}{(i-1)!}, \tag{A.7}$$
$$\psi_k = \mathcal{P}_1 \phi_k.$$

*Furthermore, the optimal coefficients $[\mathbf{c}]_k = c_k$ and $[\mathbf{d}]_i = d_i$ satisfy the matrix equations*

$$(\mathbf{G} + n\lambda\mathbf{I})\mathbf{c} + \mathbf{F}\mathbf{d} = \mathbf{q},$$
$$\mathbf{F}'\mathbf{c} = \mathbf{0}, \tag{A.8}$$

*where $[\mathbf{G}]_{kl} = \langle \psi_k, \psi_l \rangle$, $[\mathbf{F}]_{ki} = \langle \phi_k, \chi_i \rangle$, and $[\mathbf{q}]_k = q_k$, for all $k, l = 1, 2, \ldots, n$, and $i = 1, 2, \ldots, m$.*

*Proof.* We provide a sketch of the proof for completeness. A detailed proof appears in [10]. The minimizer can be expressed as

$$\hat{u} = \sum_{i=1}^{m} d_i \chi_i + \sum_{k=1}^{n} c_k \psi_k + \rho, \tag{A.9}$$

where $\rho \in \mathcal{S}_m$ is orthogonal to $\chi_1, \ldots, \chi_m, \psi_1, \ldots, \psi_n$. Then the cost functional defined in (A.5) becomes

$$\frac{1}{n} \|\mathbf{q} - (\mathbf{G}\mathbf{c} + \mathbf{F}\mathbf{d})\|^2 + \lambda \left( \mathbf{c}'\mathbf{G}\mathbf{c} + \|\rho\|^2 \right), \tag{A.10}$$

and thus $\rho = 0$. By differentiating with respect to $\mathbf{c}, \mathbf{d}$ we get the system of (A.8). $\square$

*Algorithm 6.* The optimal coefficients $\mathbf{c}$ and $\mathbf{d}$ are given by

$$\mathbf{c} = \mathbf{M}^{-1}\left(\mathbf{I} - \mathbf{F}\left(\mathbf{F}'\mathbf{M}^{-1}\mathbf{F}\right)^{-1}\mathbf{F}'\mathbf{M}^{-1}\right)\mathbf{q},$$

$$\mathbf{d} = \left(\mathbf{F}'\mathbf{M}^{-1}\mathbf{F}\right)^{-1}\mathbf{F}'\mathbf{M}^{-1}\mathbf{q}, \tag{A.11}$$

with $\mathbf{M} = \mathbf{G} + n\lambda\mathbf{I}$. Alternatively,

$$\mathbf{c} = \mathbf{Q}_2\left(\mathbf{Q}_2'\mathbf{M}\mathbf{Q}_2\right)^{-1}\mathbf{Q}_2'\mathbf{q},$$

$$\mathbf{d} = \mathbf{R}^{-1}\mathbf{Q}_1'\left(\mathbf{q} - \mathbf{Mc}\right), \tag{A.12}$$

where $\mathbf{F} = (\mathbf{Q}_1 : \mathbf{Q}_2)\left(\begin{smallmatrix}\mathbf{R}\\\mathbf{0}\end{smallmatrix}\right)$ is the QR decomposition of $\mathbf{F}$, $\mathbf{Q}_1$ is $n \times m$, $\mathbf{Q}_2$ is $n \times (n - m)$, $\mathbf{Q} = (\mathbf{Q}_1 : \mathbf{Q}_2)$ is orthogonal, and $\mathbf{R}$ is an $m \times m$ upper triangular matrix.

*Proof.* Equations (A.11) come from the minimization of (A.10) with respect to $\mathbf{c}$ and $\mathbf{d}$. For (A.12), note that since $\mathbf{F}'\mathbf{c} = \mathbf{0}$ it must be that $\mathbf{Q}_1'\mathbf{c} = \mathbf{0}$. Since $\mathbf{Q}$ is orthogonal, $\mathbf{c} = \mathbf{Q}_2\boldsymbol{\gamma}$ for some $(n - m)$-dimensional vector $\boldsymbol{\gamma}$. Equations (A.12) follow easily by substituting in the first equation in (A.11) and multiplying with $\mathbf{Q}_2'$. □

*Remark 5.* The two formulas for the coefficients (A.11) and (A.12) give exactly the same results. According to [10] the formulas given by (A.12) are more suitable for numerical work than those of (A.11). Note however, that when $m = 1$, the matrix $\mathbf{F}$ becomes a vector and (A.11) can be simplified since the term $\mathbf{F}'\mathbf{M}^{-1}\mathbf{F}$ becomes a scalar.

## Acknowledgments

## References

[1] A. A. Lazar, "Multichannel time encoding with integrate-and-fire neurons," *Neurocomputing*, vol. 65-66, pp. 401–407, 2005.

[2] A. A. Lazar and L. T. Tóth, "Perfect recovery and sensitivity analysis of time encoded bandlimited signals," *IEEE Transactions on Circuits and Systems I*, vol. 51, no. 10, pp. 2060–2073, 2004.

[3] A. A. Lazar and E. A. Pnevmatikakis, "Faithful representation of stimuli with a population of integrate-and-fire neurons," *Neural Computation*, vol. 20, no. 11, pp. 2715–2744, 2008.

[4] A. A. Lazar and E. A. Pnevmatikakis, "A video time encoding machine," in *Proceedings of the 15th IEEE International Conference on Image Processing (ICIP '08)*, pp. 717–720, San Diego, Calif, USA, October 2008.

[5] P. N. Steinmetz, A. Manwani, and C. Koch, "Variability and coding efficiency of noisy neural spike encoders," *BioSystems*, vol. 62, no. 1–3, pp. 87–97, 2001.

[6] G. Gestri, H. A. K. Mastebroek, and W. H. Zaagman, "Stochastic constancy, variability and adaptation of spike generation: performance of a giant neuron in the visual system of the fly," *Biological Cybernetics*, vol. 38, no. 1, pp. 31–40, 1980.

[7] F. Gabbiani and C. Koch, "Coding of time-varying signals in spike trains of integrate-and-fire neurons with random threshold," *Neural Computation*, vol. 8, no. 1, pp. 44–66, 1996.

[8] A. A. Lazar and E. A. Pnevmatikakis, "Consistent recovery of stimuli encoded with a neural ensemble," in *Proceedings of IEEE International Conference on Acoustics, Speech, and Signal Processing (ICASSP '09)*, pp. 3497–3500, Taipei, Taiwan, April 2009.

[9] A. Berlinet and C. Thomas-Agnan, *Reproducing Kernel Hilbert Spaces in Probability and Statistics*, Kluwer Academic Publishers, Dordrecht, The Netherlands, 2004.

[10] G. Wahba, *Spline Models for Observational Data*, SIAM, Philadelphia, Pa, USA, 1990.

[11] V. N. Vapnik, *Statisitical Learning Theory*, Wiley-Interscience, New York, NY, USA, 1998.

[12] A. R. C. Paiva, I. Park, and J. C. Príncipe, "A reproducing kernel hilbert space framework for spike train signal processing," *Neural Computation*, vol. 21, no. 2, pp. 424–449, 2009.

[13] I. Dimatteo, C. R. Genovese, and R. E. Kass, "Bayesian curve-fitting with free-knot splines," *Biometrika*, vol. 88, no. 4, pp. 1055–1071, 2001.

[14] R. E. Kass and V. Ventura, "A spike-train probability model," *Neural Computation*, vol. 13, no. 8, pp. 1713–1720, 2001.

[15] N. Aronszajn, "Theory of reproducing kernels," *Transactions of the American Mathematical Society*, vol. 68, no. 3, pp. 337–404, 1950.

[16] R. A. Adams, *Sobolev Spaces*, Academic Press, New York, NY, USA, 1975.

[17] P. Dayan and L. F. Abbott, *Theoretical Neuroscience: Computational and Mathematical Modeling of Neural Systems*, MIT Press, Cambridge, Mass, USA, 2001.

[18] P. Lichtsteiner, C. Posch, and T. Delbruck, "A $128 \times 128$ 120 dB 15 $\mu$s latency asynchronous temporal contrast vision sensor," *IEEE Journal of Solid-State Circuits*, vol. 43, no. 2, pp. 566–576, 2008.

[19] J. W. Pillow, L. Paninski, V. J. Uzzell, E. P. Simoncelli, and E. J. Chichilnisky, "Prediction and decoding of retinal ganglion cell responses with a probabilistic spiking model," *The Journal of Neuroscience*, vol. 25, no. 47, pp. 11003–11013, 2005.

[20] M. Reed and B. Simon, *Methods of Modern Mathematical Physics. Vol. 1: Functional Analysis*, vol. 1, Academic Press, New York, NY, USA, 1980.